

# NUMERICAL SIMULATION OF CHOKED GAS-SOLID TWO-PHASE FLOW WITH HEAT TRANSFER IN PIPES

Mofreh H. Hamed  
 Mechanical Power Engineering Department  
 Faculty of Engineering, Menoufiya University  
 Shebin El-kom, EGYPT  
 E-mail: [Mofrehhh@yahoo.com](mailto:Mofrehhh@yahoo.com)

**Abstract:** - A mathematical model for choked gas-particle two-phase flow in pipes is presented. The model takes into account the momentum and heat transfer between the gas and the particle phases. The wall surface roughness and the coupling effect are also considered. In addition effects of loading coefficient, initial slip velocity coefficient, wall roughness and particle diameter on the choked of gas-solid two-phase flow are investigated. The present study covers two separate cases firstly the case of no heat transfer (adiabatic flow), and secondly the case of heat transfer (heating flow). The Results of present predictions are compared with the published data and a reasonable degree of agreement is obtained. The validation has proved that the present model adequately predicts the basic flow parameters in many aspects of the flow of gas-solid mixtures at low and high speeds. The present results show that choked pipe length and the outlet parameters of adiabatic gas-particles flow show extreme difference from those under heating flow conditions. The results also show that the loading coefficient, slip velocity coefficient, particle size and pipe roughness have a strong effect on the choked pipe length and outlet parameters of gas-particles flow.

**Key-Words:** Gas-solid suspension, pipe, heat transfer, friction, roughness, choking phenomenon, coupling parameters.

## 1 Introduction

The injection of powder into metals under the conditions of gas flow velocity nearly up to sound velocity is becoming increasingly important for steel refining processes. The influence of particle size distribution on high-speed flow of gas solid suspensions in a pipe has been studied experimentally and theoretically by Mobbs et al. [1]. They have concluded that, the method described for computing the variation of gas and solid temperatures and velocities along the pipe, starting from the measured pressure distribution, has been shown to give good agreement with experimental results. They have also concluded that, the assumption of a constant velocity and temperature lags cannot be justified under choking conditions. Thakurta et al. [2] have used direct simulation to compute numerically the thermophoretic deposition rate of small particles of turbulent channel flow. A steady state one dimensional flow model at a very low velocity has been presented by Irene et al. [3-4]. Numerical simulation of gas-solid two-phase flow in a two dimensional channel was given by [5-8]. In these studies, some effects such as coupling effect and velocity lag are absent. The modeling of gas-particles flows in horizontal channels with different wall roughness was made by Sommerfeld et al. [7-9] and Eskin, [10]. While Modeling dilute gas-particles flows in constant area lance with heating and friction was made by Han et al. [11].

The survey of literature reveals that most of the previous studies neglect the effects of thermal radiation, heat transfer to the wall, and coupling effect between gas and particle phases. Therefore, the aim of this study is to

investigate the effect of these parameters on the flow of gas-solid in pipes. In addition, the effects of some parameters such as, particle diameter, loading coefficient, wall roughness, inlet flow velocity and slip velocity coefficient on the flow of gas-solid in pipes are also investigated.

## 2 Mathematical Model

In order to study the choked phenomenon in gas-solid flow in pipes, a quasi-one dimensional situation has been considered as shown in Fig. (1).

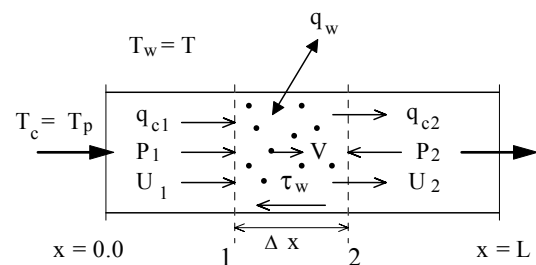


Fig. 1 Duct geometry and control volume

### 2.1 Basic assumptions

Though a simple mathematical model is introduced, the essential physical features are retained. The following assumptions are considered:

- a- The flow is one-dimensional and steady.
- b- The particles are spherical in shape.
- c- The radiative properties of gas and particles are gray.
- d- The particle density is constant, ( $\rho_p = \text{constant}$ ).

e- The heat transfer between the pipe wall and particles is negligible.

## 2.2 Governing equations

Considering the central surface shown in Fig. (1), the governing equations for both continuous phase (nitrogen) and discrete phase (SiCa powder), coupling parameters and complementary equations can be derived according to the basic laws of fluid mechanics as reported in [4, 12] as follows,

### 2.2.1 Continuous Phase

#### Continuity equation

The continuity equation for the continuous phase can be written as,

$$\frac{1}{A} \frac{\partial}{\partial x} (\alpha_c \rho_c U A) = S_{\text{mass}} \quad (1)$$

where,  $S_{\text{mass}}$  is the mass coupling parameter

#### Momentum equation

The momentum equation for the continuous phase can be expressed as,

$$\frac{1}{A} \frac{\partial}{\partial x} (\alpha_c \rho_c U^2 A) = -\alpha_c \frac{\partial P}{\partial x} + \alpha_c \rho_c g - \frac{1}{R_h} \tau_w + S_{\text{mass}} \cdot V + S_{\text{mom}_p} \quad (2)$$

where,  $S_{\text{mom}_p}$  is the momentum coupling parameter.

#### Energy equation

The differential form of the total energy equation for the continuous phase is,

$$\frac{1}{A} \frac{\partial}{\partial x} [\alpha_c \rho_c U A (h_c + \frac{U^2}{2})] = -\frac{q'_w}{R_h} - \frac{1}{A} \frac{\partial}{\partial x} (A q'_c) + \alpha_c \rho_c g U - \frac{P}{A} \frac{\partial}{\partial x} (\alpha_p V A) + S_{\text{mass}} \cdot (h_s + \frac{V^2}{2}) + S_{\text{energy}_p} \quad (3)$$

where,  $S_{\text{energy}_p}$  is the energy coupling parameter and  $q'_c$  is the effective heat transfer through both phases across surface 1. In most applications, the heat transfer through both surfaces 1 and 2 is small compared with the enthalpy flux. While,  $q'_w$  is the heat transfer to the wall.

### 2.2.2 Discrete Phase

#### The particle velocity equation

$$\text{The equation of motion for a particle in a gas is,} \\ \frac{dV^2}{dx} = \frac{2 \cdot C_D}{\tau_v} (U - V) + 2g - 4f_s \frac{V^2}{D_p} \quad (4)$$

where,  $(\tau_v = \rho_p D_p^2 / 18\mu_c)$  is defined as the velocity response time.

#### The particle temperature equation

The equation for particle temperature, assuming the temperature is uniform throughout the particle and including the radiative heat transfer is,

$$V \cdot \frac{dT_p}{dx} = \frac{Nu}{2 \cdot \tau_T} (T_c - T_p) - \frac{6 \cdot \sigma \cdot \epsilon}{D_p \cdot C_s \cdot \rho_p} (T_p^4 - T_w^4) \quad (5)$$

where,  $(\tau_T = \rho_p D_p^2 C_s / 12k_c)$  is defined as the thermal response time.

The particle Nusselt number, Nu can be calculated as reported in [1, 11 and 12].

$$Nu = 2.0 + 0.6 Re_p^{1/2} Pr^{1/3}, \quad 1 \leq Re_p \leq 70000 \\ Nu = 2.0, \quad Re_p < 1 \quad (6)$$

where,  $Re_p$  is defined as,

$$Re_p = (|U - V| \rho_c D_p / \mu_c)$$

### 2.2.3 Coupling Parameters

An important concept in the analysis of two-phase flow is to consider the coupling parameters effect between two phases. If the flow of one phase affects the other while there is no reverse effect, the flow is said to be one-way coupling. When a mutual effect exists between the two phases, the flow is called two-way coupling.

The momentum coupling source term due to the reverse effect of particles is,

$$S_{\text{mom}_p} = \frac{Z_L M'_c C_D (V - U)}{\tau_v \cdot V \cdot A} \quad (7)$$

where,  $Z_L$  is defined as the ratio between the particle mass flow rate and continuous mass flow rate,  $(M'_p / M'_c = (\alpha_p A V \rho_p) / (\alpha_c A U \rho_c))$

The energy coupling source term for the total energy equation evolves from convective heat transfer and the work done due to particle drag. The coupling source term due to convective heat transfer from the particles to the gas phase in the control volume is,

$$S_{\text{energy}_p, \text{conv.}} = \frac{Nu \cdot c_p \cdot M'_c \cdot Z_L}{3 \tau_v \cdot Pr \cdot V \cdot A} (T_p - T_c)$$

The work done due to particle drag is,

$$S_{\text{energy}_p, \text{drag}} = S_{\text{mom}_p} \cdot V$$

Then energy coupling is the sum of the two terms,

$$S_{\text{energy}_p} = S_{\text{energy}_p, \text{conv.}} + S_{\text{energy}_p, \text{drag}} \quad (8)$$

### 2.2.4 Complementary Equations

Equations (1) to (5) form a set of differential equations. In order to solve this set of equations several complementary equations, definitions and empirical correlations, are required.

1- Generally, the total friction is defined as the sum of the gas and the particle friction coefficients, which is expressed as [11],

$$f = f_c + \frac{\lambda}{1 - \lambda} f_s \quad (9)$$

Continuous phase friction  $f_c$ , can be represented with the Darcy-Weisbach friction factor and as reported in [13] by,

$$f_c = \frac{0.25}{\left[ 0.434 \ln \frac{RR}{3.7} + \frac{5.74}{Re^{0.9}} \right]^2}$$

where, RR is the ratio between the wall roughness heights to pipe diameter. While, Re is the continuous phase Reynolds number and defined by,

$$Re = \frac{U \rho_c d}{\mu_c}$$

In addition, the friction factor between particles and the wall of the pipe as reported in [11] is,

$$f_s = 1.0503 \cdot Fr_p^{-1.831}$$

Where,  $Fr_p$  is the particle Froude number and written as,

$$Fr_p = \frac{V}{(g \cdot d)^{0.5}}$$

2- Since the volume fraction of the dispersed phase and the continuous phase is unity, the continuous phase volume fraction is:

$$\alpha_c = (1 - \alpha_p) \quad (10)$$

3- The drag factor  $C_D$  can be expressed as reported in [1, 13 and 14] by,

$$\begin{aligned} C_D &= 1.0, & Re_p < 0.1 \\ C_D &= 1.0 + 0.15 Re_p^{0.67}, & 0.1 < Re_p \leq 800 \\ C_D &= 1.0 + \frac{Re_p^{2/3}}{6}, & 800 < Re_p \leq 1000 \\ C_D &= 0.0183 Re_p, & 1000 < Re_p \leq 3 \times 10^5 \end{aligned} \quad (11)$$

4- The equation of state for the gas phase is written as;

$$P = \rho_c R_c T_c \quad (12)$$

### 2.3 Initial and boundary conditions

In the present numerical analysis, calculations have been carried out for a gas-particle flow composed of nitrogen and SiCa powder.

#### 2.3.1 Initial conditions

The initial values of gas density, gas volume fraction and particle velocity are as follows,

$$\rho_{co} = \frac{P_o}{R_c T_{co}}, \quad \alpha_{co} = \frac{1}{1 + \frac{\lambda}{1 - \lambda} \cdot \frac{\rho_{co} \cdot U_o}{\rho_p \cdot V_o}}, \quad S_{V_o} = \frac{V_o}{U_o} \quad (13)$$

The gas temperature varies approximately from 273 °C to 527°C. Within this temperature range, the properties of nitrogen such as, specific heat and Prandtl number are approximately constant, while the other properties are taken as a function of temperature as reported in [15].

#### 2.3.2 Boundary conditions

The heat transfer per unit length from the wall to the gas is given as a function of pipe wall temperature and is expressed as in [4, 13] by,

$$q'_w = Stn \cdot c_p (T_w - T_c) \frac{4A}{d_h} \cdot \rho_c U \quad (14)$$

where,  $Stn$  is the Stanton number defined as in [4, 11] by,

$$Stn = \frac{h_{pipe}}{\rho_c U c_{pc}}$$

In the regime of well-developed turbulence, the relation between the coefficient of heat transfer between inner wall of the pipe and gas flow ( $h_{pipe}$ ), and friction factor  $f_c$ , can be expressed accurately with the dimensionless quantity as reported in [11] as,

$$\frac{h_{pipe}}{\rho_c U c_{pc}} = \frac{f_c}{2} \quad (15)$$

When the pipe wall is insulated such that the operating condition of the flow is adiabatic,  $q'_w = 0.0$ . Otherwise it is specified as a function of the pipe wall temperature using Eq. (14). The temperature of the inner wall of the pipe can be calculated according to [11] by,

$$T_w = 400 + 873 \cdot (x/L)^{2.4691}$$

### 2.4 Solution procedure

The physical parameters of the gas-particle flow at any section are respectively,  $\rho_c, U, T_c, P, \alpha, V, T_p$ . The solution for the system of equations, Eqs. (1-5) with the help of coupling equations (7-8) and complementary equations (9-12) are solved numerically by using an iterative approach. This approach is a marching solution in which the inlet conditions are specified and the computer program calculates the flow properties in the duct cell by cell. In the case of subsonic flow, the iteration is continued until the pressure or velocity no longer changes with continued iterations and the procedure is repeated until the end of the duct. While for the case of high velocity (choking phenomenon) is acquired, the gas velocity is just equal to the speed of sound, and the corresponding length of the duct at this time is named as critical duct length. In this case, the Mach number will not be changed. Therefore, the critical duct length can be determined at the choking condition which is defined by,  $|M - 1| \leq 10^{-3}$ . Here  $M$  is the exit Mach number.

### 3 Results and Discussion

The developed model has been designed in order to facilitate the study of many aspects of the flow of gas-solid mixtures at high speeds. Although the theoretical results have covered a wide range of gas flow rates and solids loadings, only a sample of typical results have been presented here. The continuous phase flow through a duct of 6 cm diameter is nitrogen with initial pressure, temperature and velocity of 7 bar, 400 K and 100 m/sec respectively. While the discrete phase flow is SiCa powder of density 3540 kg/m<sup>3</sup> and is charged with the flow of nitrogen through the pipe at different loading coefficients. The SiCa powder has different diameters and has also the same gas temperature but with different initial velocities depending up on the initial slip velocity coefficient which is varied from 0.2 to unity. In each case, the effects of loading coefficient  $Z_L$ , particle diameter  $D_p$ , initial slip velocity coefficient  $S_{V_o}$ , and wall roughness on the flow behaviour, the computed choked pipe length  $L_{ch}$ , outlet gas velocity ( $U_e$ ), outlet particle velocity ( $V_e$ ), and outlet particle volume fraction ( $\alpha_p$ ) are shown in Figures (2-12).

Firstly, the variations of the gas velocity, gas pressure, particle velocity, particle volume fraction and gas and particle temperatures in the case of heat transfer (heating flow) along the pipe axis at different loading coefficients,  $Z_L$  respectively are presented in Fig (2). It

can be seen that as the loading coefficient increases, the gas and particles velocities are increased and the flow is choked rapidly as shown in Fig. (2.a & b). Consequently, the required pipe length for choking flow is decreased. It is necessary to point out, that the gas temperature in the case of heat transfer (heating flow) increasing to maximum value then decreases which is referred to the friction effect near the pipe outlet as shown in Fig. (2.c).

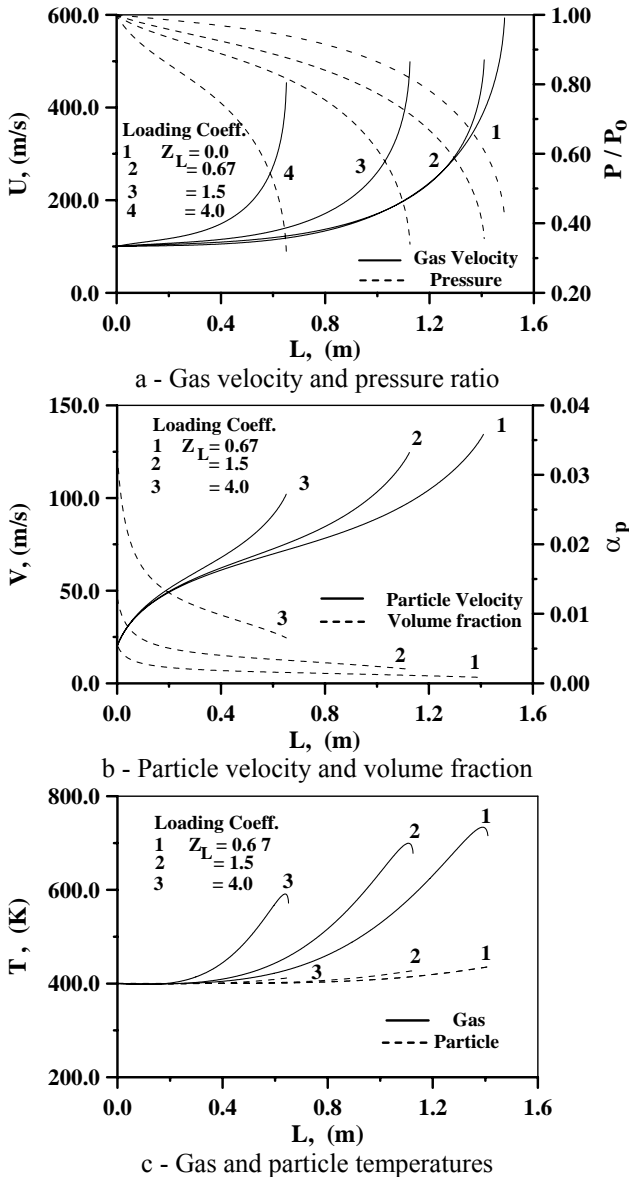


**Fig. 2** Effect of loading coefficient,  $Z_L$  on the characteristics of two-phase flow of nitrogen-SiCa powder. ( $D_p = 240 \mu m$ ,  $S_{V_0} = 0.2$ ,  $WR = 50 \mu m$ )

Figures (3 & 4) present the variation of the outlet gas velocity, outlet particle velocity, outlet particle volume fraction in the case of no heat transfer (adiabatic conditions) and also in the case of heat transfer (heating flow) for different loading coefficients,  $Z_L$  respectively. From the figures it can be seen that as the loading coefficient increases, the outlet gas velocity decreases and the flow is choked rapidly. Also the results show that the gas flow is close to choke in a small pipe length in the

case of heating flow compared with that in the case of adiabatic flow. This could be attributed to the heat transfer from the wall to the gas. Based on the present results, it can be estimated that the critical pipe length (choked length) in adiabatic and heating flow conditions in the case of gas flow without SiCa powder ( $Z_L=0.0$ ) or neglecting the coupling effect is greater than that required for nitrogen-SiCa powder for any loading coefficients as shown in Figures (2 - 4). Also it evidence to conclude that the critical pipe length (choked length) in adiabatic flow is approximately two times longer than that required in heating flow. In addition, in the case of heating flow, the outlet gas velocity is higher compared with that in the case of adiabatic flow for the same inlet conditions as shown in Figures (3 & 4). On the contrary, the outlet particle velocity is lower except in the case of zero loading. This may be due to the decrease in critical pipe length in the case of heating flow so, that the acceleration effect of particle is decreased as well. The outlet volume fraction of the particles ( $\alpha_p$ ) increases due to the deceleration of the particles and the fact that the mass particle flow rate is constant as shown in Figures (3 & 4). This is because increasing the loading coefficient, the required acceleration of the particles extracts momentum from the gas and eventually increases the pressure drop.

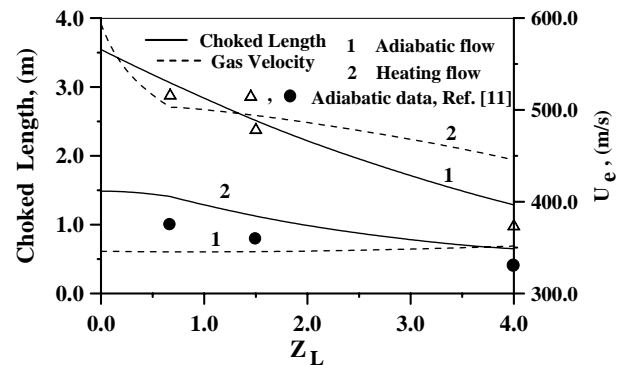


**Fig. 3** Effect of loading coefficient  $Z_L$ , on choked pipe length and outlet gas velocity.

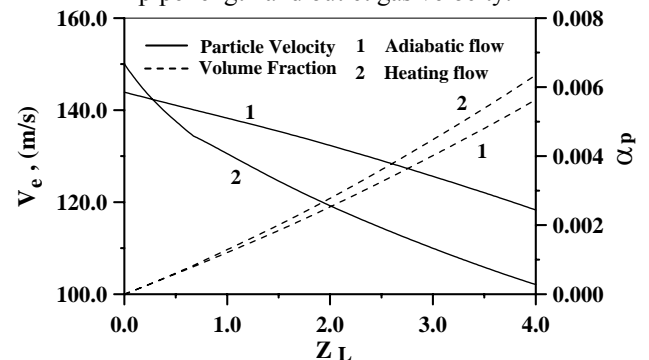


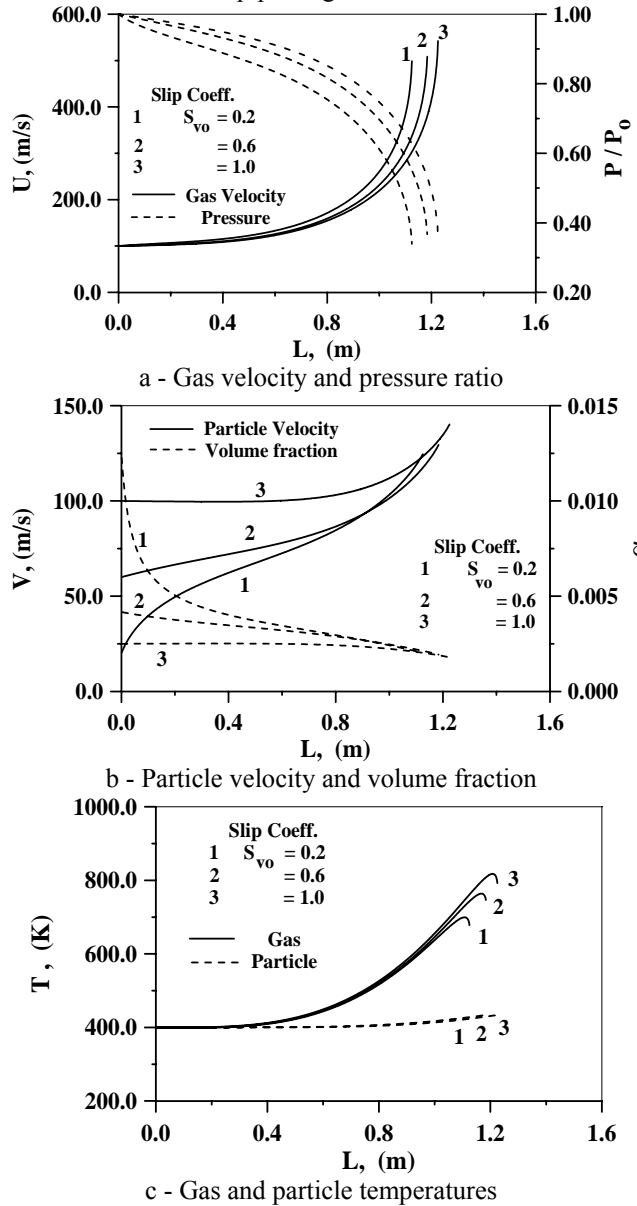
**Fig. 4** Effect of loading coefficient  $Z_L$ , on outlet particle velocity and volume fraction.

### Model Validation

To validate the present model, a comparison between the predicted choked pipe length and outlet gas velocity and published data reported in [11], is shown in Fig. (3). The calculations were carried out at the same conditions reported in [11], (adiabatic flow). The

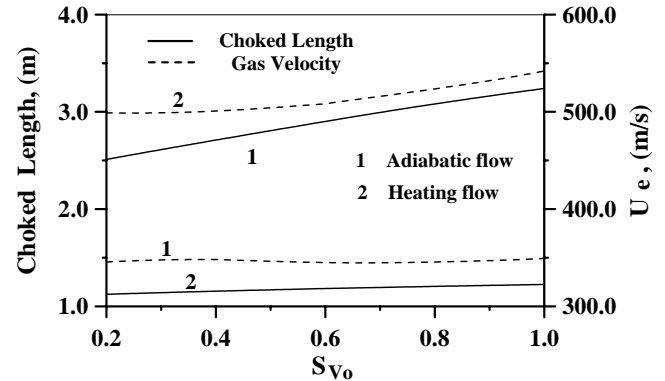
comparison shows a satisfactory agreement between the present model and published data. The discrepancy between the present results and that of [11] may be due to the wall roughness and the heat radiation which have not been considered in [11].

Figure (5) indicates the variations of the gas velocity, gas pressure, particle velocity, particle volume fraction and gas and particle temperatures in the case of heating flow along the pipe axis at different initial velocity slip coefficient respectively. It is noticed from the plots that in the case of equal initial gas and particle velocities (no slip,  $S_{vo}=1$ ), the gas velocity increases rapidly while the particle traveling approximately with constant velocity along the pipe except near the pipe outlet. This because the absence of momentum transfer. The figures also indicate that as the initial slip velocity coefficient decreases the critical pipe length decreases.



**Fig. 5** Effect of initial velocity slip coefficient,  $S_{vo}$  on the characteristics of two-phase flow of nitrogen-SiCa powder. ( $D_p = 240 \mu m$ ,  $Z_L = 1.5$ ,  $WR = 50 \mu m$ )

Figures (6 & 7) indicate the behavior of the outlet parameters of gas and particles in the case of adiabatic and heating flow conditions respectively for different initial velocity slip coefficient,  $S_{vo}$ . It is noticed from the figures that increasing the value of initial velocity slip coefficient the choked pipe length increases. This because the presence of momentum transfer as a result of increasing  $S_{vo}$ . Also it is clear that in the case of adiabatic flow the choked length increases with a higher rate compared with that in the case of heating flow.



**Fig. 6** Effect of  $S_{vo}$  on choked pipe length and outlet gas velocity.

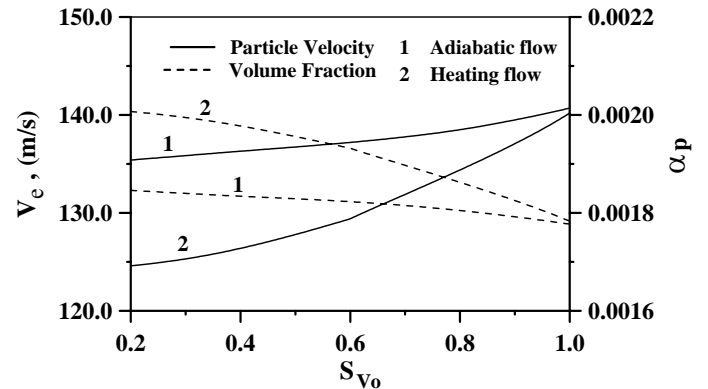


**Fig. 7** Effect of  $S_{vo}$  on outlet particle velocity and volume fraction.

The effect of particle diameter  $D_p$ , on the behavior of the gas-particle two-phase flow in the case of adiabatic and heating flow conditions is shown in Figures (8-9) respectively. The figures show that heavier particles are strongly affected by gravity. Therefore, with increasing the particle size, the particle inertia increases but the particle velocity decreases.

Plots of Fig. (10) show the variation of the gas-particle two-phase flow parameters in the case of heating flow conditions along the pipe axis with different wall roughness. It is obvious that the wall roughness has a strong effect on the gas and particle behaviour. It can be also seen that increasing the wall roughness, will increase the slip velocity coefficient and consequently decreased the pipe choked length. This is caused mainly by an increase in the momentum loss for the particle phase. It is also noticed that the magnitude of the maximum

temperature decreases, as the wall roughness increases, while the local gas temperature increases along the pipe.

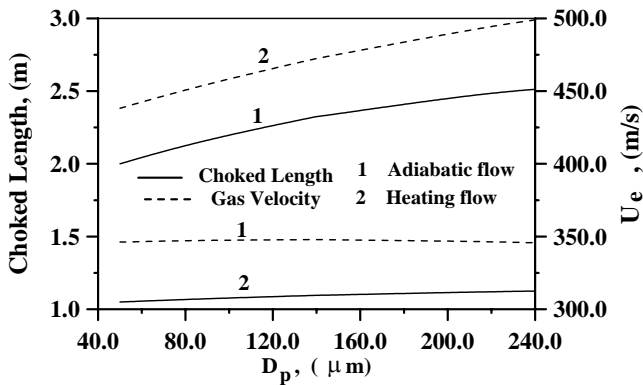


Fig. 8 Effect of  $D_p$ , on choked pipe length and outlet gas velocity.

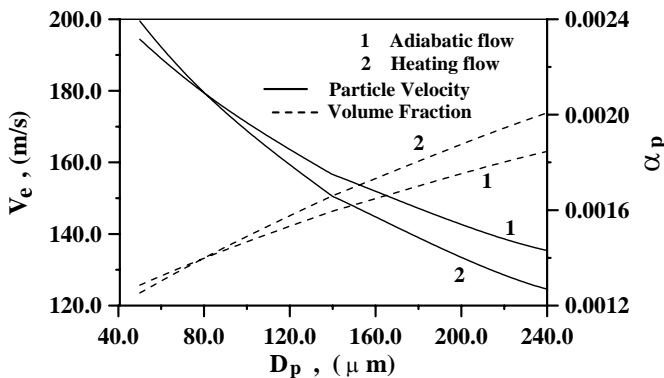
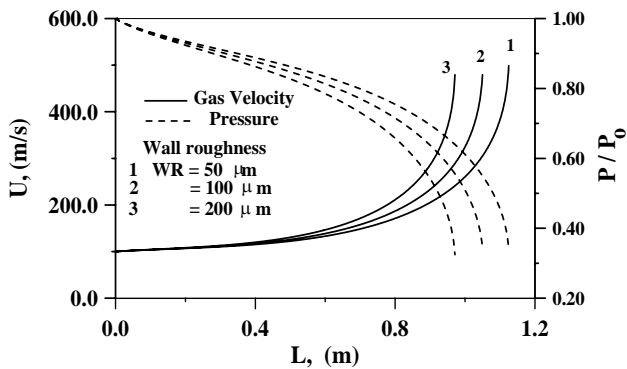
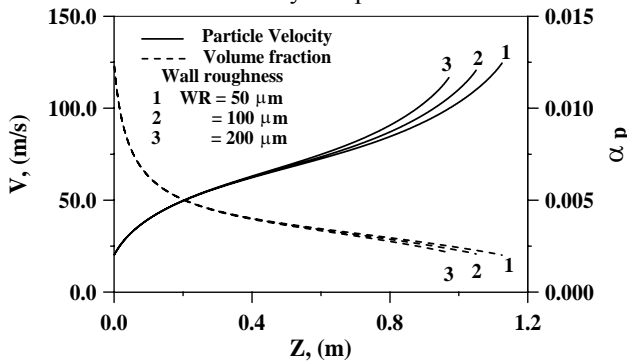


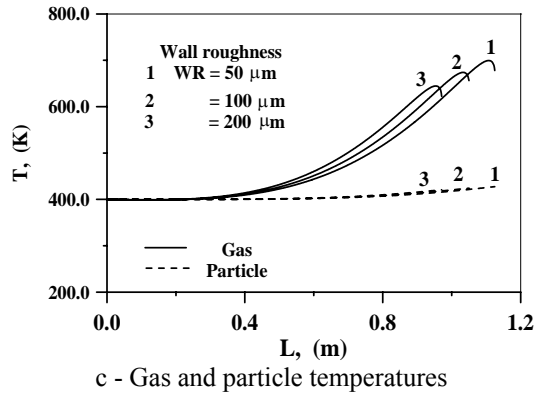
Fig. 9 Effect of  $D_p$ , on outlet particle velocity and volume fraction.



a - Gas velocity and pressure ratio



b - Particle velocity and volume fraction



c - Gas and particle temperatures

Fig. 10 Effect of duct wall roughness, WR on the characteristics of two-phase flow of nitrogen-SiCa powder. ( $D_p=240 \mu\text{m}$ ,  $Z_L=1.5$ ,  $S_{V0}=0.2$ )

Figures (11-12) show the effect of wall roughness on the outlet conditions of gas-particles two-phase flow in the case of adiabatic and heating flow conditions respectively. It is obvious that the wall roughness strongly affecting the gas and particle behaviour in the case of adiabatic conditions. It can be also seen that increasing the wall roughness, increased the slip velocity coefficient. This is caused mainly by an increase in the momentum loss for the particle phase.

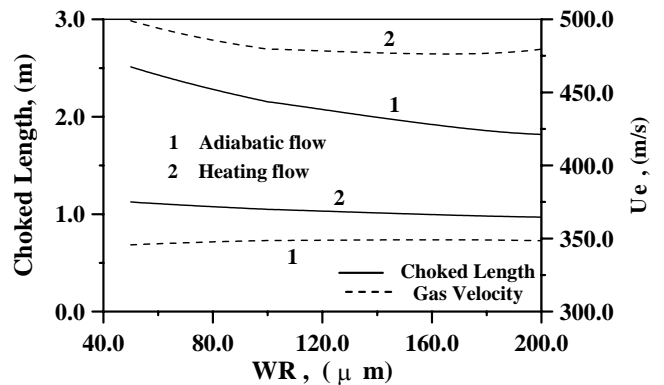


Fig. 11 Effect of wall roughness WR, on choked pipe length and outlet gas velocity.

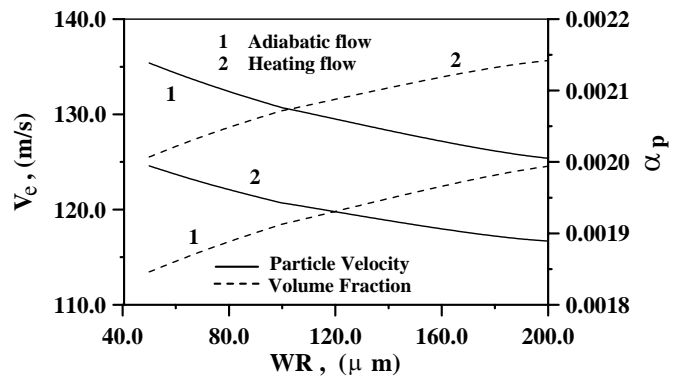


Fig. 12 Effect of wall roughness WR, on outlet particle velocity and volume fraction.

#### 4 Summery of Conclusions

From the obtained results the following conclusion can be drawn:

- The validation has proved that the present model adequately predicts the basic flow parameters in many aspects of the flow of gas-solids mixtures at high speeds.
- The choked duct length and the outlet parameters of adiabatic gas-particle flow show extreme difference from those under heating flow conditions.
- The loading coefficient, slip velocity coefficient, particle size and duct roughness have a strong effect on the choked pipe length and outlet parameters of gas-particles flow.

#### NOMENCLATURE

$A$	area,	$m^2$
$C_{pc}$	specific heat of gas phase,	$J.kg^{-1}.K^{-1}$
$C_s$	particle specific heat,	$J.kg^{-1}.K^{-1}$
$d$	pipe diameter,	$m$
$D_p$	particle diameter,	$m$
$f$	friction coefficient,	-
$C_D$	particle-gas drag coefficient,	-
$g$	gravity acceleration,	$m.s^{-2}$
$h$	enthalpy,	$J.kg^{-1}$
$k_c$	gas thermal conductivity,	$W.m^{-1}.K^{-1}$
$L$	pipe length,	$m$
$L_{ch}$	choked pipe length,	$m$
$M_c'$	gas mass flow rate,	$kg.s^{-1}$
$M_p'$	particles mass flow rate,	$kg.s^{-1}$
$Nu$	Nusselt number,	-
$P$	pressure,	$N.m^{-2}$
$R_c$	gas constant,	$J.kg^{-1}.K^{-1}$
$R_h$	hydraulic radius,	$m$
$Re$	Reynolds number,	-
$S_V$	slip velocity coefficient, $(V/U)$ ,	-
$Stn$	Stanton number,	-
$T$	temperature,	$K$
$U$	gas velocity,	$m.s^{-1}$
$V$	particle velocity,	$m.s^{-1}$
$WR$	wall roughness height,	$\mu m$
$X$	axial length,	$m$
$Z_L$	loading coefficient,	-

#### Geek Letters

$\alpha$	volume fraction,	-
$\Delta x$	increment in distance,	$m$
$\varepsilon$	emissivity,	-
$\lambda$	coefficient used in Eq. (5), $[Z_L/(Z_L+1)]$ ,	-
$\sigma$	Stephan - Boltzman constant,	$W.m^{-2}.K^{-4}$
$\mu$	air viscosity, $\mu_c = \mu_o \sqrt{T_o/T_c}$	$N.s.m^{-2}$
$\rho$	density,	$kg.m^{-3}$
$\tau_T$	thermal response time,	$s$
$\tau_V$	velocity response time,	$s$
$\tau_w$	wall shear stress,	$N.m^{-2}$

#### Subscripts

$c$	continuous phase
$co$	inlet condition of continuous phase
$e$	outlet
$o$	initial
$p$	particle

$s$	particle surface
$vo$	initial velocity slip coefficient
$w$	wall

#### REFERENCES

- [1] Mobbs F. R., H. M. Bowers, D. M. Riches, and B. N. Cole, "Influence of particle size distribution on the high-speed flow of gas-solid suspensions in a pipe," Proc Instn Mech Engrs, Vol. 184, Pt 3C paper 9, 1970.
- [2] Thakurta, D.G., M. Chen, J. B. McLaughlin, and K. Kontomaris, "Thermophoretic Deposition of Small Particles in a Direct Numerical Simulation of Turbulent Channel Flow ", International Journal of Heat and Mass Transfer, Vol. 41, No. 24, pp. 4167-4182, 1998.
- [3] Irene Borde and Avi Levy, Steady state one dimensional flow model for a pneumatic gryer, Chemical Engineering and Processing, Vol. 38, pp. 121-130, (1999).
- [4] Irene Borde, Avi Levy, David J. Mason, and David levi-Hevroni, Drying of wet solid in a steady state one dimensional flow, Powder Technology, Vol. 95, pp. 15-23, (1998).
- [5] Jianfa Cao, and Goodarz Ahmadi, Gas-particle two-phase turbulent flow in horizontal and inclined ducts, International Journal of Engineering Science, Vol. 38, pp. 1961-1981, (2000).
- [6] Tsuji, Y., Morikawa, Y., Tanaka, T., Nakatsukasa, N., and Nakatani, M., Numerical simulation of gas-solid two-phase flow in a two dimensional horizontal channel, Int. J. Multiphase Flow, Vol. 13, No. 5, pp. 671-684, (1987).
- [7] Sommerfeld M., S. Lain and J. Kussin, Experimental studies and modeling of four-way coupling in particle-laden horizontal channel flow, Proc. 2 nd Int. Symp. on Turbulence and Shear Flow Phenomena, Stockholm, 27-29 June 2001.
- [8] Sommerfeld M., S. Lain and J. Kussin, Analysis of transport effects of turbulent gas-particle flow in a horizontal channel, Proceeding of International Conference on Multiphase Flow, New Orleans, ICMF, 2001.
- [9] Sommerfeld M., Theoretical and experimental modeling of particulate flows, Overview and Fundamentals, Part I and II, Lecture Series 2000-06, von Karman Institute for Fluid Dynamics, Germany, April 3-7, 2000.
- [10] Eskin, D., Modeling dilute gas-particle flows in horizontal channels with different wall roughness, Chemical Engineering Science, Vol. 60, Issue 3, pp. 655-663, February 2005.
- [11] Han, T., A. Levy, and Y. Peng, Model for dilute gas-particle flow in constant-area lance with heating and friction, Powder Technology, Vol. 112, pp. 283-288, (2000).
- [12] Sommerfeld M., Crowe C. and Tsuji M., Multiphase flows with droplets and particles, CRC Press LLC, 1998.

- [13] Browne, L. W. B., Deposition of particles on rough surfaces during turbulent gas-flow in a pipe, Atmospheric Environment, Vol. 8, Issue 8, pp. 801-816, August 1974.
- [14] Kladas, D. D. and Deorgiou, D. P., A relative examination of  $C_D$ -Re relationships used in particle trajectory calculations, ASME J. of Fluids Engineering, Vol. 115, pp. 162-165, (1993).
- [15] William, C. Reynolds, Thermodynamic properties in SI, graphs, tables and computational equations for forty substances, Published by, Stanford University, Stanford CA 94305, January, 1979.